Dijlah Journal of Engineering Science (DJES) Vol. 3, No. 3, August, 2026, pp. 102-115
ISSN: Printed: **3078-9656, Online: 3078-9664**, paper ID:190

Advanced NARMA-L2 Based Control Strategy for an Ethylene Dichloride Cracking Reactor

Senaa Mahmoud Mashaan[1], Duraid Fadhil Ahmed[2]
[1] Department of Chemical Engineering, University of Tikrit, Iraq
[2] Professor, Department of Chemical Engineering, University of Tikrit, Iraq

Article history:

Received: Apr., 15, 2026
Revised: May.,18, 2026
Accepted: Aug.,10 2026
.

Keywords:

EDC thermal cracking, NARMA-L2, neural control, nonlinear reactor, dynamic simulation, PID control, VCM production.

ABSTRACT

The performance of the EDC Thermal Cracking Reactor study for VCM is doing quite well. The VCM that has been designed is good. A nonlinear dynamic model has been developed for studying the performance in open-loop and closed-loop system response to nonlinear change in feed temperature and feed flow rate. MATLAB/Simulink was used to design and simulate a model. Thus, as the feed temperature rises, the exit gas temperature increases to a value slightly above the target. Conversely, when the feed temperature falls, the exit gas temperature slightly dips below the target. Eventually, the exit gas and feed temperature attain their steady states with no permanent error. (16 words) Changes in flow rate also affect temperature, and the system achieves different times. Additionally, controllers were developed using the NARMA-L2 framework including PI, PID, and neural network controller. The system was assessed with respect to various controllers. Improvement shown in the handle of the thermal cracking reactor of nonlinear behavior. NARMA-L2 takes minimum settling time and lesser overshoot. It controls interference better.

Corresponding Author:
Senaa Mahmoud Mashaan

Duraid Fadhil Ahmed, Professor, Department of Chemical Engineering, University of Tikrit, Iraq
sm230019en@st.tu.edu.iq

1-Introduction

The overall industrial manufacturing process uses a thermal cracking furnace which is very important. The pyrolysis of a larger ethylene dichloride monomer is utilized for producing any size or type of vinyl chloride monomers. Vinyl chloride monomer is produced by thermal cracking 1,2-dichloroethane in a furnace. The cracked gas temperature mainly relies on temperature, volumetric flow rate, and 1,2-dichloroethane concentration, while fuel gas flow rate is a controllable variable A perfect cracked gas temperature profile along coil reactor can help achieve maximum yield of desired olefin and minimum cost of reactor de-coking down time [1]. Both the coke yield and the coke formation rate increase with increasing cracked gas temperature. Radiation is the common data that combines all the other pieces together furnace combustion shock component and chimney. The firebox, or radiation section, has a number of burners and tube sheets. Endothermic process is when heat-consuming fuels are subjected to endothermic reaction. Most industrial uses rely primarily on natural gas, while some companies produce hydrogen from their chlor-alkali plants[2]. Due to the high temperature characterization of this region, heat transfer in this region mainly takes place by radiation. The furnace's thermal degradation of EDC produces HCl and vinyl chloride monomer (VCM) as one of their primary products. It starts with the reaction of the carbon-chlorine bond involving the homolytic cleavage of carbon-chlorine bond[3]. The first-order free-radical chain mechanism is followed during this process. Usually, the cracking temperature is maintained at about 550 degree Celsius to avoid unwanted by-products. A hard-sphere collision occurs when particles collide, and energy transfer to the environment occurs through a particle-wall collision process. Chromium-nickel alloys are widely employed as furnace tube materials because of their ability to withstand high temperatures and abrasive environments. The convection section is where heat recovery occurs. The combustion gas outflow from the radiation section takes place through the shock section due to the operation of a flow splitter. Consequently, flue gases are released into the surrounding environment with the chimney. During the convection phase, the EDC is heated to its boiling temperature and then vaporized with a very pure EDC of over 99%. As the vaporized feed emerges from the shock section, it returns to the furnace, where it meets a superheating to a cracking reaction temperature, usually within the range of 400 to 430°C. In this phase, heat travels through flue gases via convection and from the combustion chamber through radiation[4].

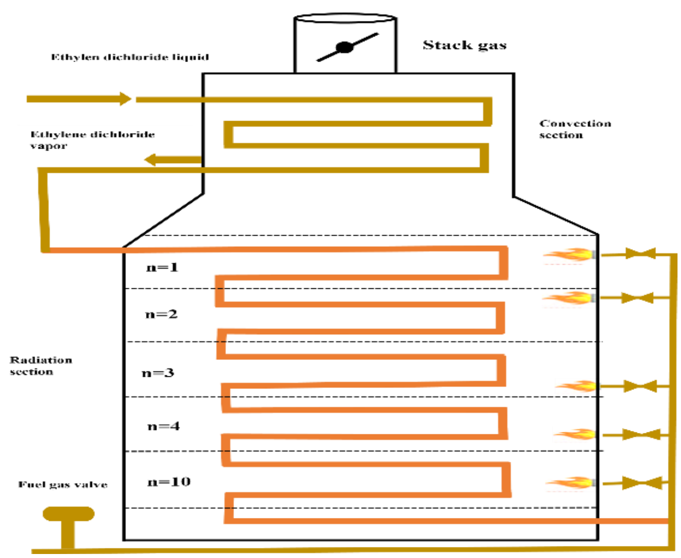

Figure 1: An example of a thermal cracking furnace for ethylene dichloride.

By changing the fuel gas consumption in its furnace, one can control the exit gas temperature and the mass produced by thermal cracking. Using a PID controller on the furnace system under control gives the best steady state performance at the set point. This is achieved through the solving of the ordinary and partial differential equations of the reactor model. Even so , As of the complex spatial effects and main interactions of the reactor coil and radiating furnace wall, they are only effective in a limited range [5]. Since the design procedure is very straightforward, PID and PI controllers are very popular in process control applications.

Artificial Neural Networks (ANN) are computer applications that employ the application of identification complex controls, models or systems. Their modeling is inspired by human brain. Dozens of papers, with experimental and theoretical evidence, argued in favor of using neural networks in practice. Chemical processes are frequently nonlinear, multivariate, and sensitive to significant changes in variables. Thus, recurrent neural networks can be used. RNNs are an example of used to approximate which is not easily represented by models. The production process, which creates vinyl chloride monomer from ethylene dichloride, is inherently non-linear and temperature-sensitive. With a conventional controller like PID, it can be challenging to stabilize the whole plant and achieve the required yield. ANN-based controllers make for a good solution, as it can learn the input-output relations of the reactors and adapt to changing conditions of the reactor [7].For nonlinear systems, the NARMA model is used in literature as well as many neural network-based methods. At discrete times, the method accurately represents any non-linear dynamic plant at the equilibrium operating point. The original NARMA model might prove inefficient because direct implementation of it can incur high costs. To address the issue, two models NARMA-L1 and NARMA-L2 were invented so that the deployment of the model can be done without losing accuracy [8].The neural control structure NARMAL2 has become popular and may be more effective now. The main advantage of this approach is that nonlinearities are effectively managed, that is a nonlinear dynamic of a system can be transformed into a suitable form for controller design [9]. The success of the controller can be enhanced through the improvement of the output tracking and reliability performances in the presence of nonlinearity of the system.It does not have to be complicated to implement NARMA-L2 controllers. In contrast to MRAC and MPC techniques that use trained sub-models, NARMA-L2 does not employ one in order to prevent structural complexity and computation costs [10]. The development of a NARMA-L2 using serial-parallel MLP neural networks was made possible by system identification. Supervised learning strategies like BPR minimize the difference between the output produced by the neural model as well as the output of the actual plant. Upon recognizing the physical behavior, the neural model may be employed to create control laws that enhance reference trajectory tracking at the system's output with improved dynamic performance. Refer to [12].According to research work, compared to other controllers NARMA-L2 has been suggested to provide better tracking accuracy, faster settling time and lower steady state error[13].The neural network model of NARMA-L2 is thus viewed as an efficient and reliable method for intelligent control and the identification of nonlinear systems.The simple structure, great approximation capability and proved tracking behaviour of the design make a good start for complex control systems of high nonlinear engineering systems.

2- Changes to the Thermal Cracking Furnace.

The fractured gas temperature, furnace wall temperature, and tube wall temperature are interacting with each other. Thus, the dynamic modeling of a thermal cracking furnace is complex and nonlinear. Energy balances take place on the gas position , tube position , and furnace position . The broken gas mass balance and energy balance corresponding to other types of chemical reaction in the reactor [14] has non-linear partial differential equations. Via dynamic modeling analysis, evaluate the control infrastructures and state of the plant. This enables engineers to evaluate the impact of design changes without the first principles models. It is necessary to accredit a dynamic model in which the controlled variable and manipulated variable vary over time for evaluating the effectiveness of a control scheme and perfecting the starting practices of the plant [15]. The model becomes more complex when the feedstock is multicomponent due to carbon deposition on the tube walls and the many complicated thermal cracking processes taking place inside the coil. The effects of ethylene dichloride concentration and volumetric flow rate plus input temperature and fuel gas flow rate will influence gas temperature in open loop mode. Assessing the impact of the above mentioned factors can be made using sensitivity indices. According to the simulation results, the flow rate of fuel gas has the most impact because it supplies the heat that raises the wall temperature of the furnace. Heat moves from the combustion gases to the tube wall and then from the tube wall to the gas by radiation conduction and convection. As a result of the temperature rises of the gas due to a faster reaction rate, the concentrations of ethylene dichloride are being slowly depleted while, at the same time, the concentrations of vinyl chloride monomer and hydrogen chloride are increasing[15].

3-Methodolog

An enhanced comprehension of process behaviour during the manufacturing of vinyl chloride monomer (VCM) was achieved through the development of a dynamic model of the EDC thermal cracking reactor. Afterward, a MATLAB/Simulink simulation model was developed to examine the reactor's dynamic behavior under different scenarios and parameters. To control reactor outlet gas temperature, an intelligent control strategy based on a NARMA-L2 neural network controller was developed. To depict the non-linear behavior of the process controller, data is being simulated. To assess its performance, adjustments were made to the temperature setpoint, along with disturbances in the feed concentration, feed temperature, and gas flowrate.

3.1- Dynamic model

We study the overall coil reactor model which incorporates it into a dynamic model. In the model, we have the mass and energy balance equations of cracking coil reactor. The energy balances of the coil and of the oven wall are defined by ordinary differential equations, whereas the mass and energy balances of the cracked gas are defined by partial differential equations in space position and time.

Above all these are the mass and energy balance about the differential section shown in figure 2.

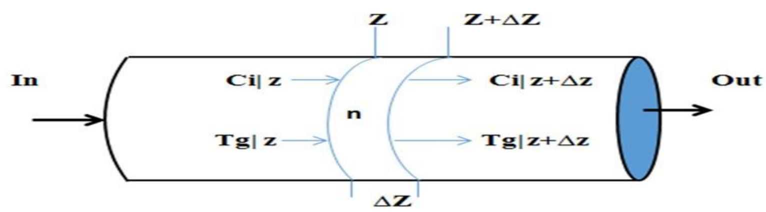

Figure 2: Input and output temperature and concentration profiles for the reactor section of length z.

The mass balance on fractured gas under unsteady state conditions is stated as follows in segment element (Δz)

$$\lim_{\Delta z=0} \frac{\partial Cin}{\partial t} = v \lim_{\Delta z=0} \frac{[ci|zn - ci|z + \Delta z]}{\Delta zn} + \lim_{\Delta z=0} \sum_{j=1}^{Nr} Sji\, rj \qquad (1)$$

Accordingly, Equation (1) is expressed as follows:

$$\frac{\partial Cin}{\partial t} = -v \frac{\partial Cin}{\partial zn} + \sum_{j=1}^{Nr} Sji\, rj \qquad (2)$$

The segment element provides insight into how energy is balanced on fractured gas in the reactor under non-steady-state condition

$$\rho_{gn} CPg_n A_c \Delta z_n \frac{\partial T_{gn}}{\partial t} = \sum_{j=1}^{Nc} Mwi\ Fi\ CPi\left[Tg_{n|zn} - Tg_{n|zn+\Delta zn}\right] + Qc_n \frac{\Delta z_n}{L_n} + A_c \Delta z_n \sum_{j=1}^{Nr} r_j\left(\Delta H_j\right) \qquad (3)$$

Equation (3) is divided by $\rho_{gn} CPg_n A_c \Delta z_n$ and Δz is taken to zero, it yields to get

$$\frac{\partial T_{gn}}{\partial t} = \frac{\sum_{j=1}^{Nc} Mwi\ Fi\ CPi}{\rho_{gn} CPg_n A_c} \frac{\partial T_{gn}}{\partial z} + \frac{Qc_n}{\rho_{gn} CPg_n\, V_{tn}} + \frac{\sum_{j=1}^{Nr} r_j\left(\Delta H_j\right)}{\rho_{gn} CPg_n} \qquad (4)$$

ISSN: Printed: **3078-9656, Online: 3078-9664**, paper ID:190

The following formulae are then used to get the reaction temperatures [17] and the heat capacity of component I [18]:

$$CPi = c_1 + c_2\left(\frac{\frac{c_3}{T_{gn}}}{\sinh\left(\frac{c_3}{T_{gn}}\right)}\right)^2 + c_2\left(\frac{\frac{c_5}{T_{gn}}}{\cosh\left(\frac{c_5}{T_{gn}}\right)}\right)^2 \tag{5}$$

$$\Delta H_{(T)} = \Delta H_{(298)} + \Delta\, CP_{(298)}(T - 298) \tag{6}$$

$$\Delta\, CP_{(298)} = \sum \text{produ}\, CP_{(298)} - \sum \text{rectant}\, CP_{(298)} \tag{7}$$

The following formulas are used to determine the cracked gas heat transfer coefficient and heat transmission from tube wall to cracked gas [19]:

$$Q_{cn} = \frac{2\pi R_3\left(T_t - T_g\right)}{\left[\frac{\ln\frac{R_3}{R_2}}{k_t} + \frac{ln\frac{R_2}{R_1}}{k_{Cok}} + \frac{1}{R_3 hg}\right]} \tag{8}$$

$$h_g = 0.023\,\frac{k_i}{D}\left(\frac{\rho_g D_v}{\mu}\right)^{0.8}\left(\frac{\mu CP_g}{k_i}\right)^{0.4} \tag{9}$$

The cracked gas represents mass and energy balances associated with the partial differential equations. Using the backward finite difference method [20], numerical solutions of the governing equations are obtained and the spatial derivatives of Ci and Tg along z are approximated.

Mass and energy balance can be done using the following equations.

To maintain the balance of mass:

$$\frac{\partial Cin}{\partial t} = -v\left[\frac{C_{in} - C_{in-1}}{\Delta zn}\right] + \lim_{\Delta z = 0}\sum_{j=1}^{Nr} Sji\, rj \tag{10}$$

The energy balance will be calculated using equation (6).

$$\frac{\partial T_{gn}}{\partial t} = \frac{\sum_{j=1}^{Nc} Mwi\, Fi\, CPi}{\rho_{gn} CPg_n A_c}\,\frac{\left[Tg_{n|zn} - Tg_{n|zn+\Delta zn}\right]}{\Delta z_n} + \frac{Qc_n}{\rho_{gn} CPg_n V_{tn}} + \frac{\sum_{j=1}^{Nr} r_j\left(\Delta H_j\right)}{\rho_{gn} CPg_n} \tag{11}$$

The equation governing the energy balance in the coil wall can be given as [11].

$$m_{tn} CP_t \frac{\partial T_{tn}}{\partial t} = Aw_n\, F\, \sigma\left(Tw_n^4 - Tt_n^4\right) - \frac{2\pi R_3\left(T_{tn} - T_{gn}\right)}{\left[\frac{\ln\frac{R_3}{R_2}}{k_t} + \frac{ln\frac{R_2}{R_1}}{k_{Coke}} + \frac{1}{R_3 hg}\right]}$$

(12)

$$m_w CP_w \frac{\partial T_w}{\partial t} = m\ fuel\ LHV - Aw\ F\ \sigma\ (Tw_n^4 - Tt\ _n^4) - Q\ fuel\ gas \qquad (13)$$

3.2- NARMA-L2 Controller

The NARMA-L2 is a complex control technique which is used in dynamic systems. It uses neural networks to manage complicated processes and simulations. Instead of just carrying out mathematical operations, the NARMA-L2 learns the behaviour of the system from data. As a result, it may be applied to systems in which PID and other classical controllers would not work effectively.

Design NARMA-L2 Neural Controller

The region of input linearization control, also known as NARMA-L2 neural controller, was considered. The method of linearizing the critique would be usable only if the exhibit of the plant could be cast into a particular canonical form. When the dynamics of a plant can be spoken to or approximated by a controlling function, the resulting control scheme is referred to as NARMA-L2 control. The primary aim of this strategy is to convert the framework's Non-Linear Flow in to Direct Flow compensating for the non-linearities in the framework. The area starts with the presentation of consort-form frameworks and demonstrates how a neural organize perceives them. This project discusses the improvement of a controller depending on the chosen neural network model...

$$u(k+1) = \frac{y(k+d) - f[y(k),\ldots,y(k-n+1),u(k),\ldots,u(k-n+1)]}{g[y(k),\ldots,y(k-n+1),u(k),\ldots,u(k-n+1)]} \qquad (14)$$

It is possible when d is greater than two.

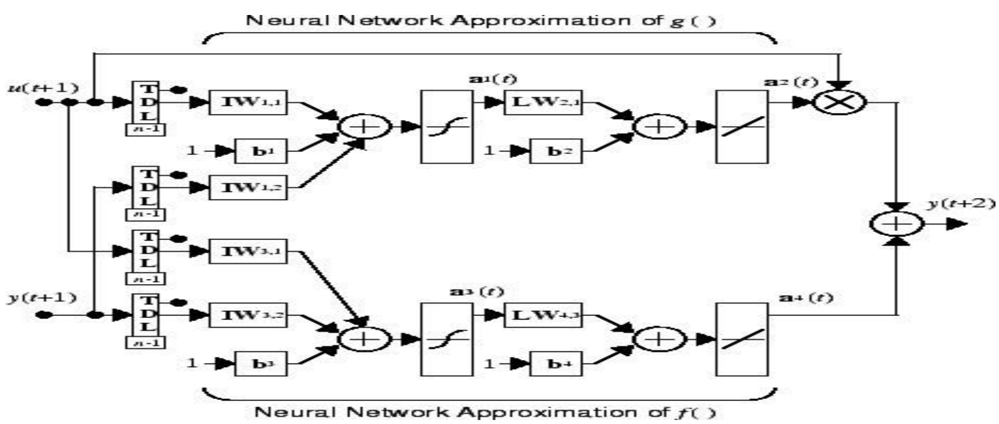

Figure 3: Identification of Narma-L2 Control via Neural Network

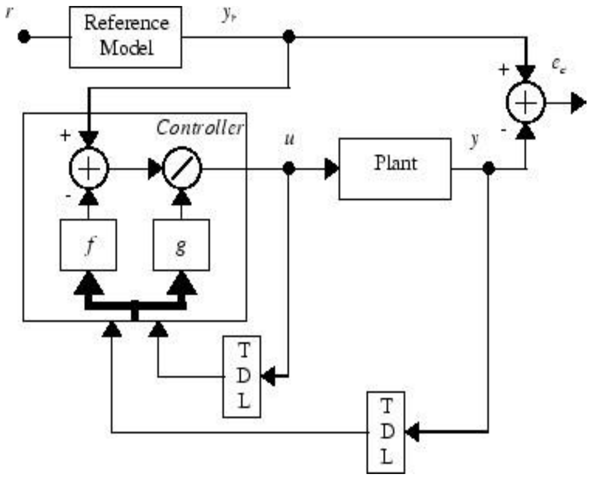

Figure 4 : Narma -L2 interface.

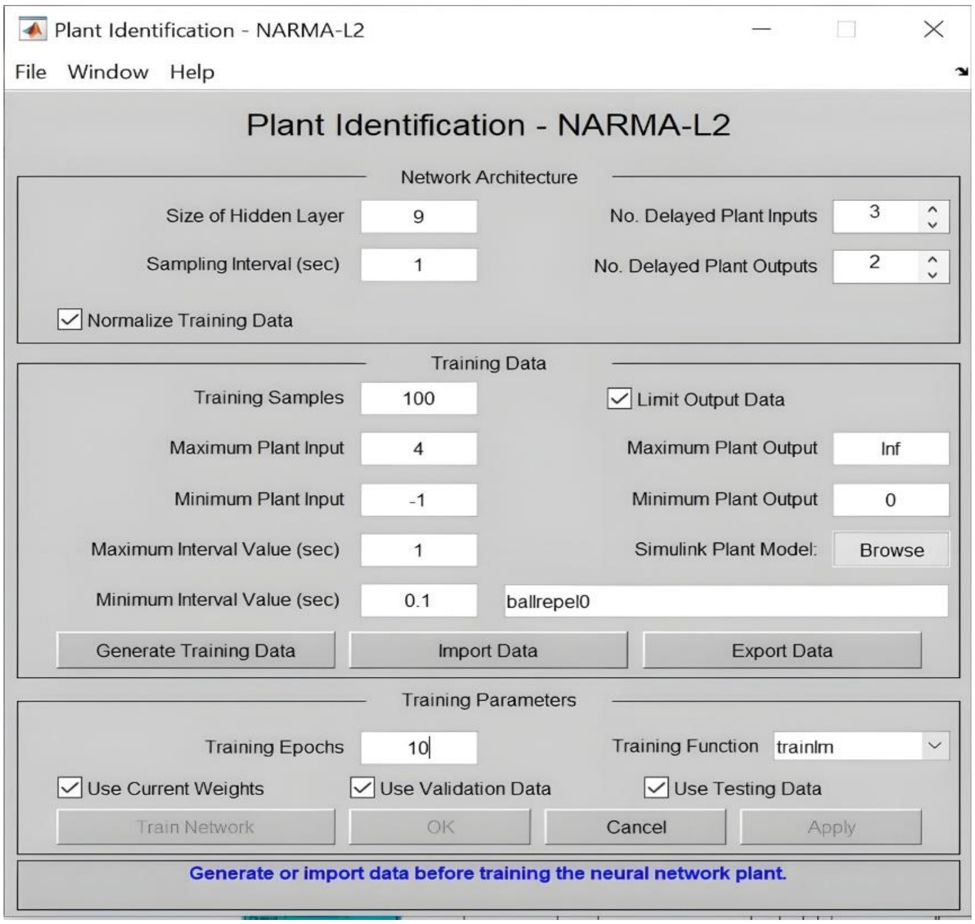

Figure 5: Designing a NARMA-L2 neural controller with a plant identification window in MATLAB/Simulink.

ISSN: Printed: **3078-9656, Online: 3078-9664**, paper ID:190

3.4- Simulation work

Designing a smart controller NARMA-L2 neural network and its implementation on output gas temperature control of ethylene dichloride thermal cracking furnace in a study. A simulation model in MATLAB/Simulink for the process architecture was created, the NARMA-L controller was used. The PI or PID linear controller is a worse choice in the presence of a vast range of the system's underlying nonlinearities.

By increasing or decreasing the fuel gas flow rate in the control scheme you control and hence can measure the output gas temperature of the furnace. The dynamic response open-loop data of the system was used to train the neural network for that system. We had to adjust the epochs, hidden layer size (14 neuron) and sampling period (0.5 s) parameters. After training, the controller was connected to a nonlinear plant. The functioning was determined through varying a step disturbance. The study of transient performance on settling time, overshoot and steady-state error reveals that the NARMA-L2 technique is superior to classical or conventional control in terms of stability and tracking..

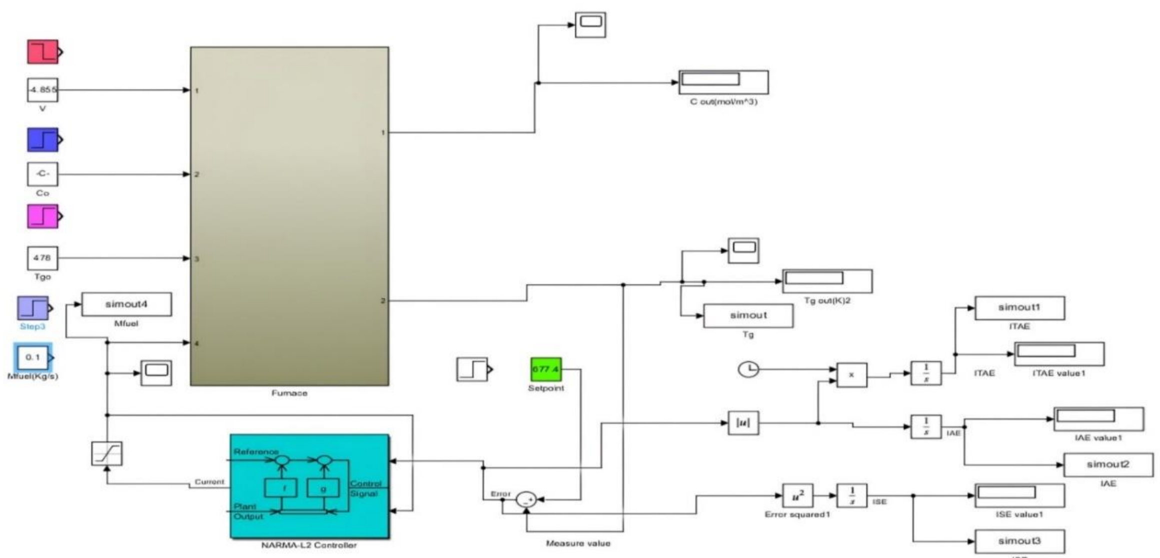

Figure 6 : Simulation Experiment of Ethylene Dichloride Thermal Cracking Furnace of Narmal 2 Controller.

4-Result And Discussion

The performance of this simulation work is validated against the results as well as industrial data from [21] for a thermal cracking furnace of ethylene dichloride. Based on the table, the actuals as compared to some simulated work exit cracked gas temperature the conversion of ethylene dichloride. How selective is vinyl chloride monomer?

Table 4. Temperature, conversion, and selectivity of outflow fractured gas are compared in simulation study.

Flexible	Real	Modelled	Variation %
Firebox and conversion	53	53.7	1.32
Selectiveness	0.99	0.97	2
The temperature of the fractured exit was°C.	494.1	500	1.1

4.1-Effect of step change Variable

The EDC feed refers to a type of changes which is a good step distubrance calculated by the system and is depicted in the system and is shown in Figure . 7. The concentration of the reactant and the reaction kinetics can suddenly raise the temperature of the exit gas from the reactor. The NARMA-L2 controller effectively adjusts the temperature to the specified setpoint. The system will oscillate, overshoot then stabilise after a few cycles..

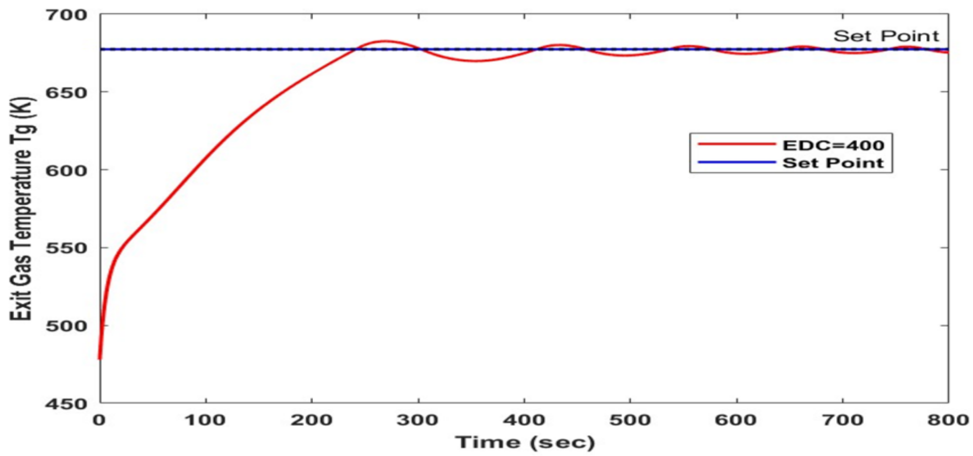

Figure 7 : Reactions to the positive step change in ethylene dichloride feed (mol/l) concentration cause NARMA exit gas temperature.

The temperature of reactor exit gas decreases remarkably for a negative step change of EDC feed concentration. As evident from the system response shown in Figure 8, the controller changes the controlled variable in order to eliminate the effect of disturbance so that the system returns to planned operating condition with minimum value of steady state error.

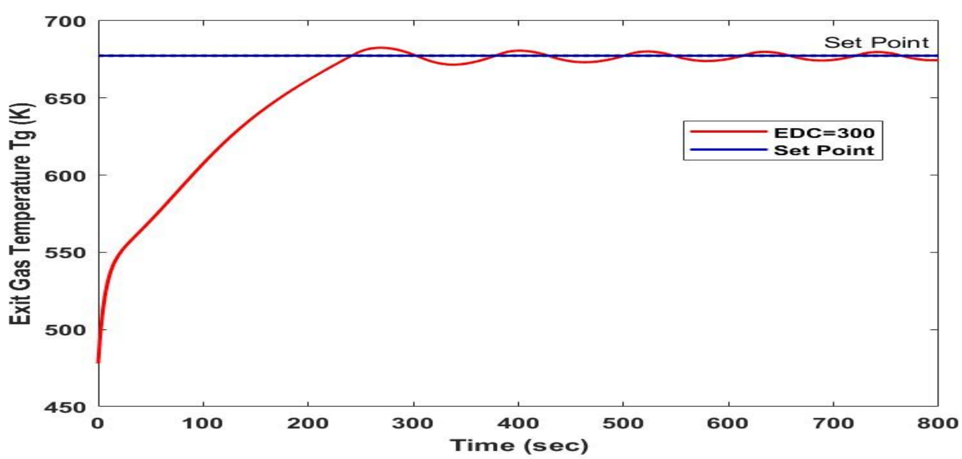

Figure 8 : The temperature response of NARMA-L2 exit gas due to a negative step change in the ethylene dichloride (mol/l) input concentration..

As shown in Figure 9, a positive step disturbance in the feed temperature causes noticeable changes in both the thermal behaviour of the reactor and the exit gas temperature. The NARMA-L2 controller has fast correction capability which reduces deviation and brings the system to set point in a very short settling time...

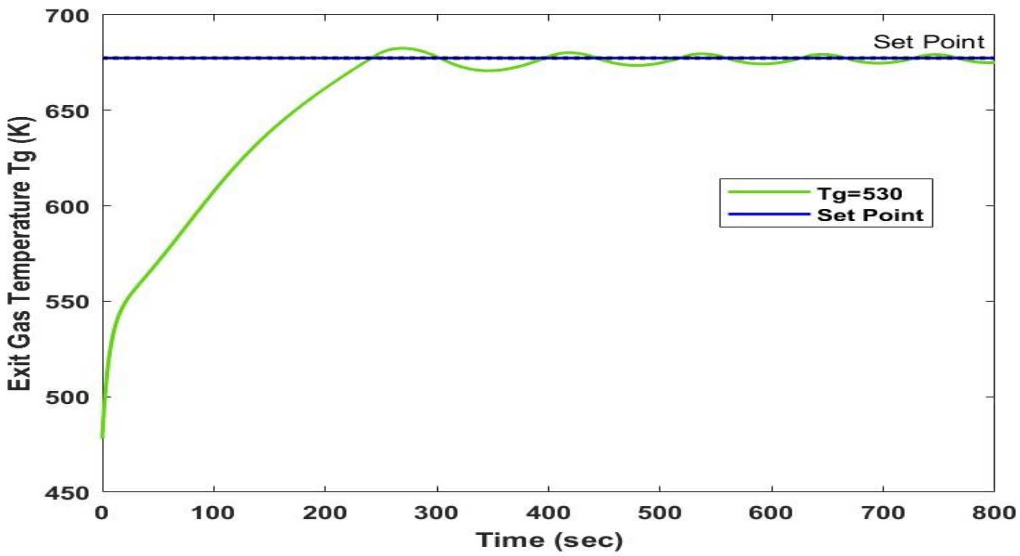

Figure 9 : The impact of a positive step change in the feed temperature on NARMA exit gas temperature

After the feed experiences an unfavorable step change in temperature, the system's reaction is shown in Figure 10. The figure demonstrates a sudden drop in intake temperature, returning to a steady state, but the controller remains stable as compensation for this disturbance.

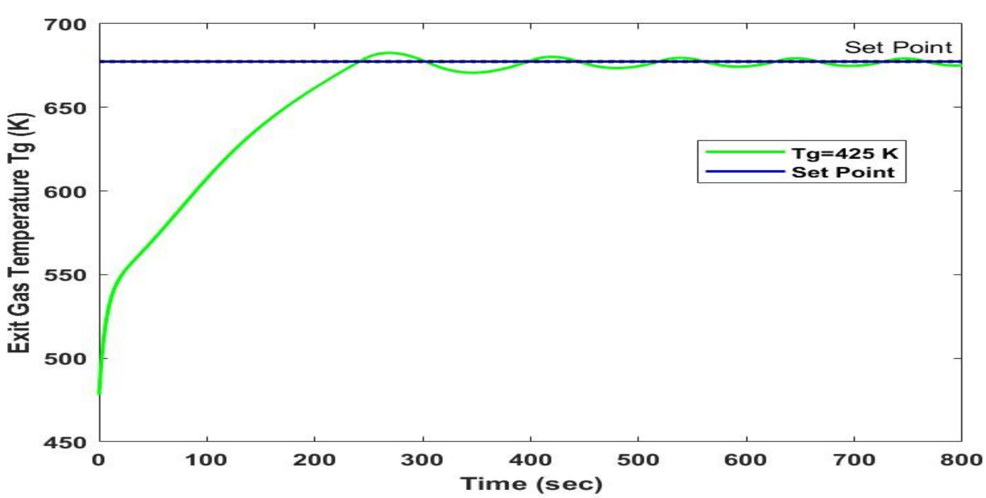

Figure 10 : NARMA-L2 exit gas Temperature response is caused by negative step change of input temperature (K).

The results for negative step disturbance illustrated in the figure 11, are seen through change in volumetric gas flow rate. The temperature of exit gas will lower in the case of a decreased flow rate which will influence its residence time and heat transfer properties in the reactor. The controller stabilizes the system around the set-point for adequate trajectory performance..

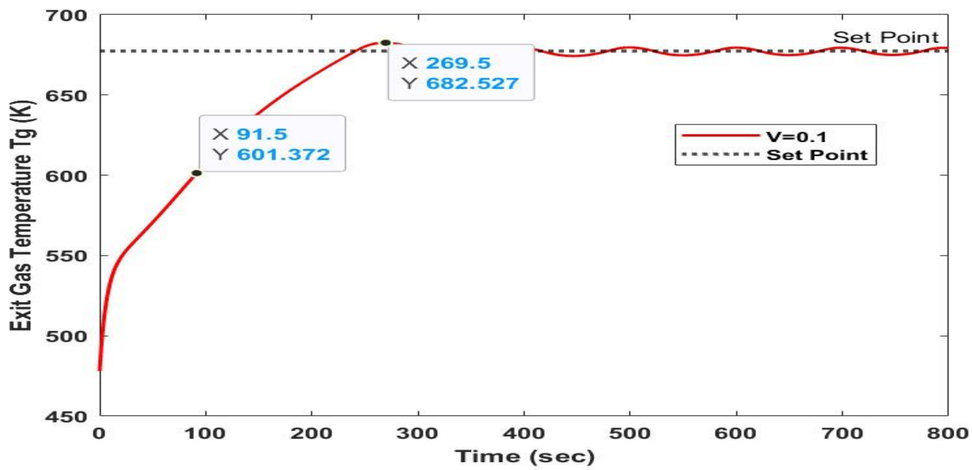

Figure 11 : When the volumetric flow rate is switched, the exit gas temperature response is observed.

As seen from figure 12, the system responds to a positive step change of the volumetric gas flow. The findings reveal that the controller suitably mitigates this disturbance so that no violations on the reactor exit temperature are detected.

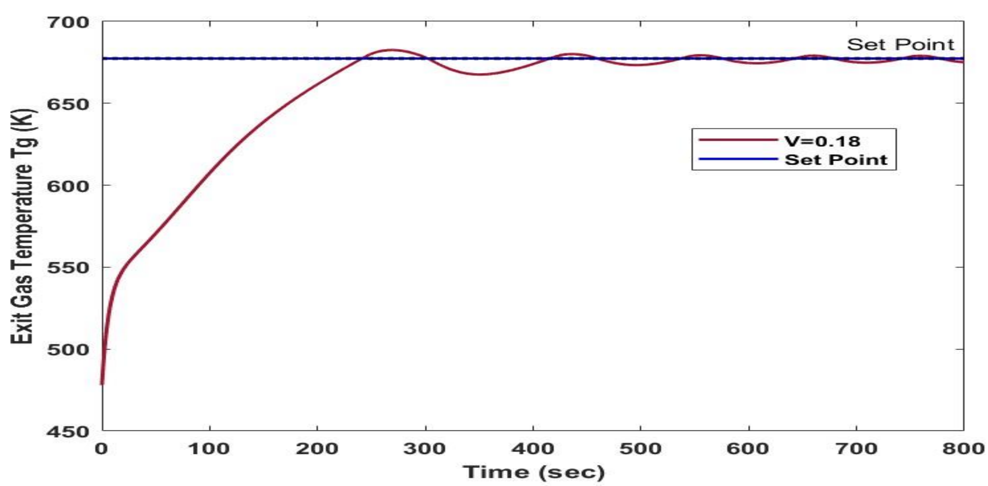

Figure 12 : An increase in the volumetric flow rate (m3/s) is a cause of NARMA exit gas temperature reaction.

Illustrated in Figure 13, taking the reactor exit gas temperature set-point, is the dynamic behaviour of NARMA-L2 controller against positive and negative step change. The set-point is originally maintained at approximately 654.8 K.

The reference temperature is increased to approximately 700 K by applying a positive step change. The controller tunes the controlled variables to increase the value of exit gas temperature to the new target..

The set-point is changed from 700 K to around 654.8 K via a negative step adjustment. By lowering the exit gas temperature and directing it toward the new operating state, the controller successfully reacts to this decline. With just slight oscillations and a little steady-state error, the response exhibits stable behavior.

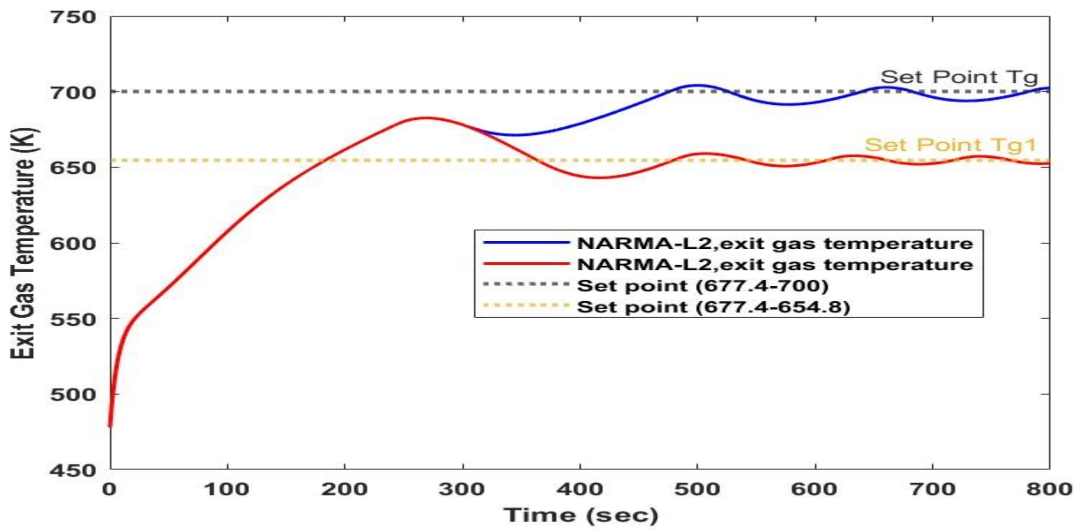

Figure 13 : The exit gas temperature in NARMA-L2 responds to respond a step change in the set point gas temperature (K) .

4.2-Comparison between Controllers

A comparative study is conducted on error-based performance measures and transient response characteristics to evaluate the efficacy of the control strategies employed. The smart control method has lesser overshoot, undershoot and total error compared to conventional controllers. The operating characteristics and performance appear identical under all conditions. The controllers displayed a variation in performance of quantitative type as shown in figures **14** and **15**. The smart controller exhibits better control performance and system dynamics as indicated by the decrease in ITAE values and IAE values with varying reactor temperatures, feed concentrations, volumetric flow rates and temperature set-point values..

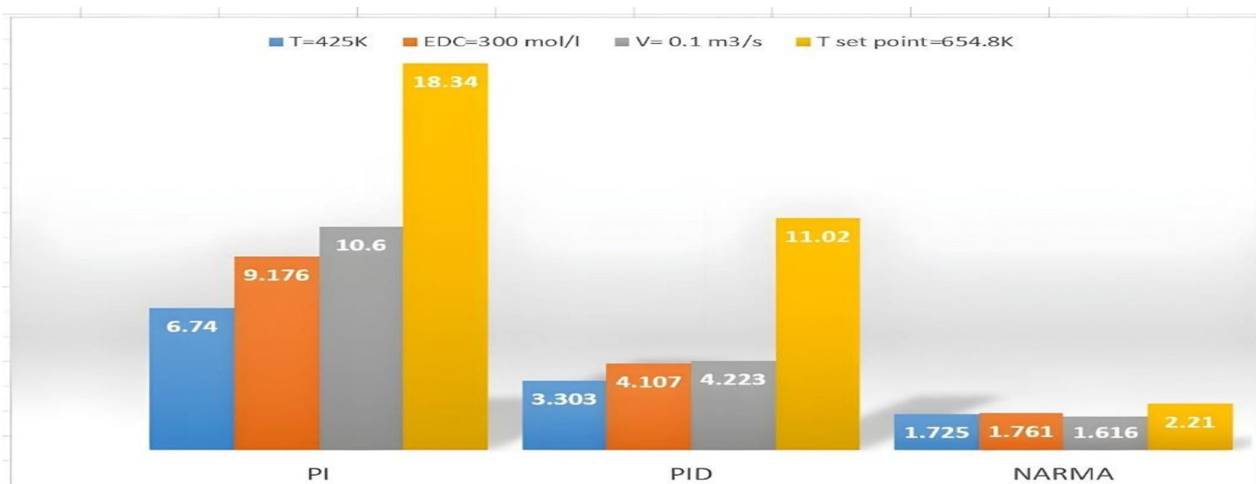

Figure 14 : Comparing the three controllers' ITAE performance indexes.

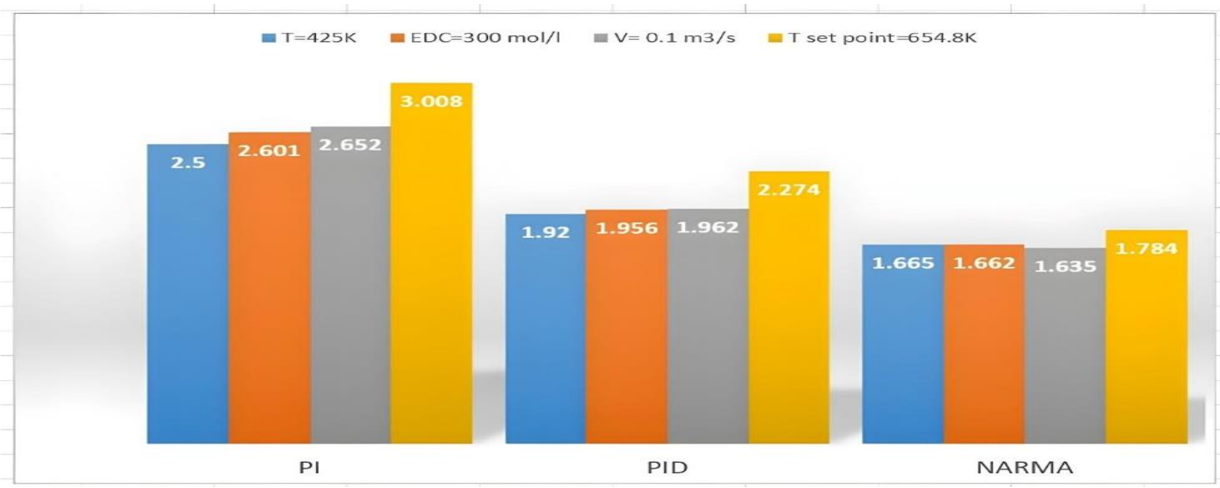

Figure 15 : IAE performance indicators for the three controllers are compared.

5- Conclusions

The data provided in the study on the contrary modelling, simulation and control of the thermal cracking furnace of EDC.

• The developed mathematical model is verified since the performance in the open-loop simulations for output cracked gas temperature, EDC conversion and selectivity is similar to that operating data in the industry.

• The PID controller settings obtained via the Ziegler-Nichols closed-loop tuning method are acceptable as they yield a satisfactory dynamic performance with small steady-state errors, reasonable settling times and small overshoot/undershoot.

• The Neural Network-based NARMA-L2 controller is a more effective controller than a standard PI and PID controller . The suggested control strategy enhanced the thermal cracking furnace performance by yielding shorter settling periods, reduced overshoot and undershoot, and reduced error indices for various types of disturbances and set-point changes..

6- Recommendations for Future Work

The following suggestions are put forth for conducting research in order to enhance the accuracy and control performance of the thermal.

1. To improve the thermal modelling of reactor tube wall energy balance calculations, the convection heat transfer component will be included.
2. The temperature functionality of the heat-producing body influences the heat capacity. Additionally, the temperature at which the production of radicals and chemical intermediates takes place.
3. The first study was concerned with how varied mechanisms influenced the performance of an ethylene dichloride thermal reactor reaction.
4. Alter operating conditions and feedstock composition range of investigation.
5. For best performance of thermal cracking, the system can control all important process variables simultaneously..

Reference:

[1] Shahrokhi M, and Ali. N. " Optimal temperature control of a propane thermal cracking reactor ". Industrial & engineering chemistry research 41(25):6572-6578, 2002.

[2] Dry, J., Lawson, B., Le, P., Osisanya, I., Patel, D., & Shelton, A. (2003). Vinyl Chloride Production. university of Oklahoma.

[3] Dreher, E. L., Beutel, K. K., Myers, J. D., Lübbe, T., Krieger, S., & Pottenger, L. H. (2014). Chloroethanes and chloroethylenes. Ullmann's encyclopedia of industrial chemistry, 5, 257-309.

[4] Choi, B. S., Oh, J. S., Lee, S. W., Kim, H., & Yi, J. (2001). Simulation of the effects of CCl4 on the ethylene dichloride pyrolysis process. Industrial & engineering chemistry research, 40(19), 4040-4049

[5] Tawai A., and Panjapornpon C. "Input–output linearizing control strategy for an ethylene dichloride cracking furnace using a coupled PDE–ODE model". Industrial & Engineering Chemistry Research, 55(3): 683–691, 2016.

Dijlah Journal of Engineering Science (DJES) Vol. 3, No. 3, August, 2026, pp. 102-115
ISSN: Printed: **3078-9656, Online: 3078-9664**, paper ID:190

[6] Abdullah, N., Yee, T. C., Mohamed, A., Mustafa, M. M., Osman, M. H., & Mohamad, A. B. (2016). Control of continuous stirred tank reactor using neural networks. Indian journal of science and technology, 9(21), 95238.
[7] Y. M. Ren, M. S. Alhajeri, J. Luo, S. Chen, F. Abdullah, Z. Wu, and P. D. Christofides, “A tutorial review of neural network modeling approaches for model predictive control,” Computers & Chemical Engineering, vol. 165, 2022.
[8] Sharma, P., 2014, NARMA-L2 Controller for Five-Area Load Frequency Control, Indonesian Journal of Electrical Engineering and Informatics, Vol. 2, No. 4, pp. 170-179.
[9] George, M., & Basu, K. P. (2012). NARMA-L2 controlled variable frequency three-phase induction motor drive. European Journal of Scientific Research, 70(1), 98-111.
[10] Al-Dunainawi, Y., Abbod, M. F., & Jizany, A. (2017). A new MIMO ANFIS-PSO based NARMA-L2 controller for nonlinear dynamic systems. Engineering Applications of Artificial Intelligence, 62, 265-275 .
[11] Zurada J. M. “Introduction to artificial neural systems”, 1992.
[12] Jeyachandran, C. and Rajaram, M., 2014, Neural Network Based Predictive, NARMA-L2 and Neuro-Fuzzy Control for a CSTR Process, Journal of Engineering and Applied Science, Vol. 5, No. 3, pp. 30-42.
[13] Putrus, K. M. (2011). Implementation of neural control for continuous stirred tank reactor (CSTR). Al-Khwarizmi Engineering Journal, 7(1), 39-55.
[14] Panjapornpon C, Patara L and Tawatchai Charinpanitkul " Control of coupled PDEs–ODEs using input–output linearization": Application to a cracking furnace. Chemical engineering science 75:144-151, 2012.
[15] Ghashghaee, M., & Karimzadeh, R. (2007). Dynamic modeling and simulation of steam cracking furnaces. Chemical Engineering & Technology: Industrial Chemistry-Plant Equipment-Process Engineering-Biotechnology, 30(7), 835-843.
[16] Joo, E., S. Park and M. Lee; “Pyrolysis Reaction Mechanism forIndustrial Naphtha Cracking Furnaces,” Ind. Eng. Chem. Res.,40, 2409–2415 (2001).
[17] H Scott, F. (2006). Elements of chemical reaction engineering: Prentice-Hall Profesional.
[18] Green, D. W., & Southard, M. Z. (2019). Perry's chemical engineers' handbook: McGraw- Hill Education.
[19] Masoumi, M., Shahrokhi, M., Sadrameli, M., & Towfighi, J. (2006). Modeling and control of a naphtha thermal cracking pilot plant. Industrial & Engineering Chemistry Research, 45(10), 3574-3582.
[20] Ingham, J., Dunn, I. J., Heinzle, E., & Ingham, J. (2000). Chemical engineering dynamics: Wiley Online Library.
[21] Nyeng I " Modeling of a 1, 2-Dichloroethane Cracker NTNU", 2015.

BIOGRAPHIES OF AUTHORS

	Senaa Mahmoud Mashaan acquired her B.Sc. She received her Bachelor’s Degree in Chemical Engineering from the College of Engineering, Tikrit University, Tikrit, Iraq in 2021. A PHD candidate in Chemical Engineering at the College of Engineering, Tikrit University, in the research stage of his master’s thesis. Her scientific investigations are concentrated on NARMA-L2-based dynamic modeling-simulation-intelligent control of EDC thermal cracking process. Using MATLAB/Simulink, the performance of thermal cracking furnace for vinyl chloride monomer (VCM) production has been simulated and analysed for the process. Her email address is **sm230019en@st.tu.edu.iq**.